INTERNATIONAL SOCIETY FOR SOIL MECHANICS AND GEOTECHNICAL ENGINEERING

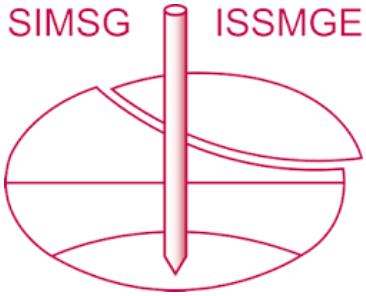

The paper was published in the proceedings of the 17th African Regional Conference on Soil Mechanics and Geotechnical Engineering and was edited by Prof. Denis Kalumba. The conference was held in Cape Town, South Africa, on October 07-09 2019.

Proceedings of the 17th African Regional Conference on Soil Mechanics and Geotechnical Engineering

Editor

S.W. Jacobsz
University of Pretoria, Pretoria, South Africa

Anisotropy effects on the undrained stability of cuts in clays

M. Mánica
National Autonomous University of México, Mexico City, Mexico

S. Conesa
Tongji University, Shanghai, China

A. Gens
Universitat Politècnica de Catalunya, Barcelona, Spain

ABSTRACT: It has long been recognised that soils are generally anisotropic with some of their properties varying depending on the direction of measurement. In particular, strength anisotropy should be a main concern in relation with the stability assessment of geotechnical cases. Nevertheless, the incorporation of this feature is rarely considered in routine slope stability analyses in spite of the fact that its absence may lead, in some cases, to an overestimation of the factor of safety. In the paper, the effects of strength anisotropy on the undrained stability of cuts in clays are examined. A literature review reveals that clays have different patterns of undrained strength anisotropy depending on their overconsolidation ratio. A constitutive model is introduced, able to account for the different observed variations of undrained strength with loading direction. A series of numerical stability analyses have been performed to explore the effects of the type of undrained strength anisotropy on the stability of cuts. The effects of slope inclination, bedding orientation, and pattern of undrained strength anisotropy on factors of safety and failure mechanisms are examined and discussed. In addition, a real case study of the failure of an underwater cut is analysed showing that undrained strength anisotropy is able to explain satisfactorily the collapse observed.

1 INTRODUCTION

Geomaterials are generally anisotropic with some of their properties varying depending on the direction of measurement (e.g. Arthur et al. 1977). In particular, strength anisotropy should be a main concern in relation to the stability assessment of geotechnical cases. Nevertheless, the incorporation of this feature is rarely considered in routine slope stability analyses in spite of the fact that its absence may lead, in some cases, to an overestimation of the factor of safety.

Two main steps are required to include strength anisotropy in our stability calculations: the first one is to establish a failure criterion introducing a dependency with the direction of loading. The second one is to include such a failure criterion into an appropriate methodology for assessing the stability such as limit equilibrium methods or limit analyses. Another appealing alternative is the use of numerical methods. For instance, the finite element method (FEM) has proved to be a reliable and robust alternative for assessing the factor of safety (FOS) of slopes (Griffiths & Lane 1999). Therefore, the use of FEM in combination with an anisotropic constitutive law constitutes an attractive possibility for the study the effect of anisotropy on the undrained stability of cuts in clays.

Early works including strength anisotropy in slope stability analyses (e.g. Chen et al. 1975) considered only a monotonic decrease of the strength between loading perpendicular and parallel to bedding. As described later, this is a typical behaviour of K_0 normally consolidated clays. However, overconsolidated clays may exhibit a quite different behaviour not yet properly considered in stability computations.

In the paper, the effects of undrained strength anisotropy on the stability of cuts in clays are examined using the FEM. A constitutive model is introduced, able to account for the different observed variations of undrained strength with the direction of loading (relative to bedding). The model is then employed in a number of stability analyses, performed to identify situations where strength anisotropy will play a major role. In addition, a real case study of the failure of an underwater cut is analysed showing that undrained strength anisotropy is able to explain satisfactorily the collapse observed.

2 UNDRAINED STRENGTH ANISOTROPY IN CLAYS

In the late 60s, Skempton & Hutchinson (1969) noted how the undrained strength of clays varies with the loading direction (Fig. 1). For normally or lightly overconsolidated clays (clay from Welland, San Francisco Bay clay, and clay from Surte in Figure 1), the

strength is highest when the major principal stress σ_1 is normal to bedding. Then, the strength either decreases monotonically with orientation or there is minimum value at an intermediate orientation but with a strength just slightly lower than for loading parallel to bedding. However, overconsolidated clays (London clay from Wraysbury and Ashford sites in Figure 1) exhibit a different pattern. The behaviour is similar to normally consolidated clays when the angle of the major principal stress and the normal to bedding is small, but then the strength rises rapidly so that the value for loading parallel to bedding can be even higher than for loading perpendicular to bedding. Skempton & Hutchinson (1969) interpreted that these high strengths for loading parallel to bedding probably reflect the high lateral in situ consolidation pressure, suggesting a progressive evolution of anisotropy with the change in overconsolidation ratio (OCR). Both types of behaviours (for normally or lightly overconsolidated and for overconsolidated clays) have been more recently confirmed using the hollow cylinder apparatus at the Imperial College, London (e.g. Nishimura et al. 2007, Zdravkovic & Jardine 2000).

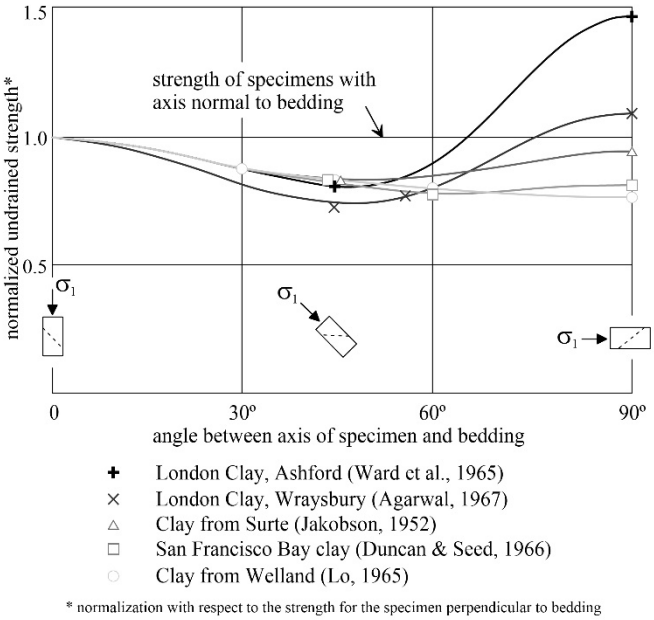

Figure 1. Normalised undrained strength variation with loading direction (modified from Skempton & Hutchinson 1969).

3 ANISOTROPIC CONSTITUTIVE MODEL

The model used is formulated within the framework of elastoplasticity. Inside the yield surface, the response is assumed linear elastic characterised by Hooke's law. As only the problem of undrained stability of cuts in clays is addressed here, the yield surface is characterised by Equation 1 corresponding to the Tresca yield function.

$$f = J\cos\theta - S_{\mathrm{u}} \tag{1}$$

where $J = \sqrt{J_2}$, J_2 is the second invariant of the deviatoric stress tensor $\mathbf{s}$, θ is the Lode's angle, and S_{u} is the undrained strength.

The anisotropic extension of the model is obtained by replacing S_{u} in Equation 1 by

$$S_{\mathrm{u}}^{*} = \Omega(\delta) S_{\mathrm{u0}} \tag{2}$$

where δ is the angle between the normal to bedding and the direction of the applied major principal stress, S_{u0} is the undrained strength measured with $\delta = 0°$, and Ω is a given function accounting for the variation of the undrained strength with the loading direction.

If $\mathbf{n}$ is the vector normal to the bedding and $\mathbf{v}$ is the direction of the major principal stress, δ can be defined as

$$\delta = \cos^{-1}\frac{|\mathbf{n}\cdot\mathbf{v}|}{|\mathbf{n}|\cdot|\mathbf{v}|} \tag{3}$$

The direction of $\mathbf{n}$ accounts for situations where the bedding plane is not horizontal with respect to the global coordinate system. In a 3D analysis, where the z axis stands for depth, the orientation of the bedding plane can be described according to Figure 2a where $\mathbf{n}$ is given by

$$\mathbf{n} = \begin{bmatrix} \sin\beta\sin\alpha \\ -\cos\alpha\sin\beta \\ \cos\beta \end{bmatrix} \tag{4}$$

In a 2D analysis, where the y axis stands for the depth, and the orientation of bedding is assumed to vary only around the direction normal to the analysis plane, $\mathbf{n}$ is defined as (Fig. 2b)

$$\mathbf{n} = \begin{bmatrix} -\sin\alpha \\ \cos\alpha \\ 0 \end{bmatrix} \tag{5}$$

For the definition of $\mathbf{v}$, the eigenproblem must be solved for the stress tensor. In the model, this is performed numerically using the Jacobi method.

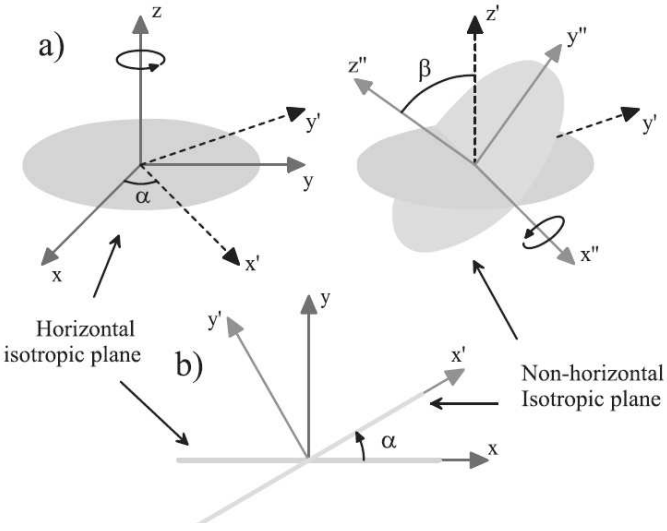

Figure 2. Orientation of the bedding plane for (a) 3D and (b) 2D problems.

The function employed as Ω should be flexible enough to accommodate the various types of undrained strength variations showed in Figure 1. Here, Ω is defined as

$$\Omega = \frac{A\mathrm{e}^{(\delta_\mathrm{m}-\delta)n}}{\left[1+\mathrm{e}^{(\delta_\mathrm{m}-\delta)n}\right]^2} + \frac{B}{1+\mathrm{e}^{(\delta_\mathrm{m}-\delta)n}} + C \quad (6)$$

where

$$\mathrm{A} = 2(e_1+1)(e_2+1)(e_1-e_2+\Omega_{90}+e_1e_2+ e_1\Omega_{90}-e_2\Omega_{90}-2e_1\Omega_\mathrm{m}+2e_2\Omega_\mathrm{m}-e_1e_2\Omega_{90}-1)/ [(e_1-e_2)(e_1-1)(e_2-1)] \quad (7)$$

$$\mathrm{B} = \frac{\Omega_{90}-\frac{Ae_1}{(e_1+1)^2}+\frac{Ae_2}{(e_2+1)^2}-1}{\frac{1}{e_1+1}-\frac{1}{e_2+1}} \quad (8)$$

$$\mathrm{C} = 1-\frac{Ae_2}{(e_2+1)^2}-\frac{B}{e_2+1} \quad (9)$$

$$e_1 = \mathrm{e}^{n(\delta_\mathrm{m}-90)} \quad (10)$$

$$e_2 = \mathrm{e}^{n\delta_\mathrm{m}} \quad (11)$$

and Ω_{90}, Ω_m, δ_m, and n are material parameters (see Conesa et al. 2018 for further details).

Examples of how Equation 6 is able to account for the types of strength variations described in section 2 are depicted in Figure 3. They correspond to the Boston blue clay (Seah 1990), an Alaskan silt (Fleming & Duncan 1990), and the London clay (Nishimura et al. 2007). The corresponding parameters are given in Table 1. These strength distributions are also employed in the analyses described in the following section.

Regarding the plastic potential function, in the absence of relevant data, it was assumed isotropic.

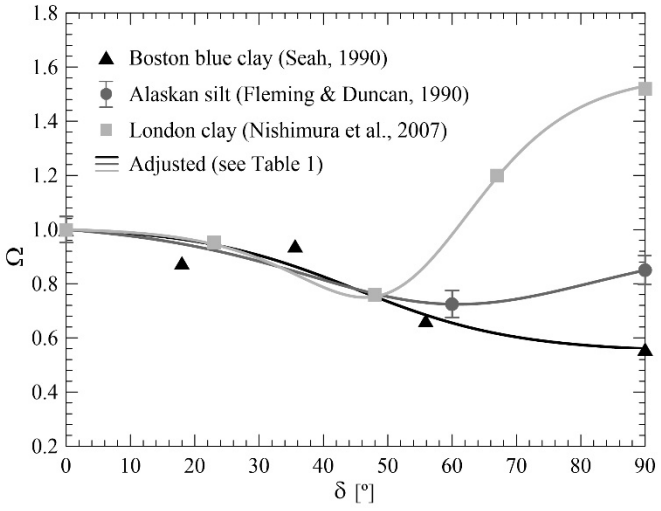

Figure 3. Observed and computed normalised undrained strength distributions.

Table 1. Parameters of the adjusted strength distributions

Parameter	Boston blue clay	Alaskan silt	London clay
Ω_{90}	0.56	0.85	1.53
Ω_m	0.78	0.73	0.79
δ_m	45°	59°	52°
n	0.08	0.06	0.11

4 STABILITY ANALYSES

A series of finite element analyses were performed, using the constitutive model described in the previous section, to assess the influence of inherent strength anisotropy on the undrained stability of cuts. Three different fine-grained materials reported in the literature were considered in the analyses, showing the different strength variations identified in section 2 (Figure 3). The main objective is to recognise situations where strength anisotropy will play a major role in the stability analysis.

4.1 *Main features of the analyses*

Figure 4 shows the geometry and main boundary conditions employed. They correspond to a 2D (plane strain) cut of height H in homogeneous soil with the firm ground located at a vertical distance H from the toe. Different slope angles θ and different orientations of the bedding α were considered.

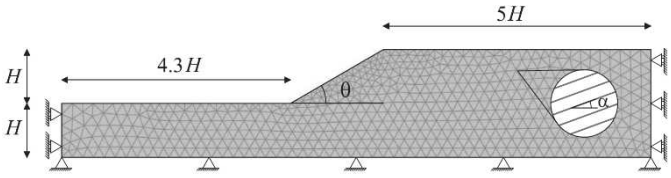

Figure 4. Geometry and boundary conditions employed.

Analyses were performed with the finite element code Plaxis (Brinkgreve et al. 2017), where the model described in section 3 was implemented. The strength reduction method was employed to determine the failure condition (Griffiths & Lane 1999). Therefore, the FOS is defined here as

$$\mathrm{FOS} = \frac{s_\mathrm{u}}{s_{\mathrm{u-f}}} \quad (12)$$

where $s_{\mathrm{u-f}}$ is the undrained strength at which failure occurs. Results were then normalised in terms of the stability number N_0 (Eq. 13).

$$\mathrm{N_0} = \frac{\mathrm{FOS}\,\gamma H}{s_\mathrm{u}} \quad (13)$$

where γ is the unit weight of the soil.

Analyses were performed first without including anisotropy, and the results were compared to Taylor's (1937) solution. Then, the strength distributions in Figure 3 were included to assess their effect on the stability analyses.

The resulting failure mechanisms are also reported below. They are represented by a continuous single

line drawn at the centre of the zone where a high displacement gradient occurs separating the stationary part of the ground and the sliding mass.

4.2 *Obtained results*

Stability numbers obtained for different inclinations of the slope are shown in Figure 5. Here, the bedding is assumed horizontal. A good agreement can be noticed between the isotropic analysis and Taylor's solution, validating the employed numerical approach. In the anisotropic analyses, the variation of N_0 with the slope inclination θ has a similar trend than the isotropic one although the magnitude is considerably different. The Boston clay lies at the bottom of the graph as the most unfavourable condition whilst London clay shows N_0 values even higher than the isotropic case for θ lower than 50°. For higher inclinations, the London clay and the isotropic case are quite similar. The Alaskan silt is found between the isotropic case and the Boston clay. It is important to notice that the effect of anisotropy reduces with θ, so that in the case of a vertical cut ($\theta = 90°$) the effect of anisotropy becomes negligible.

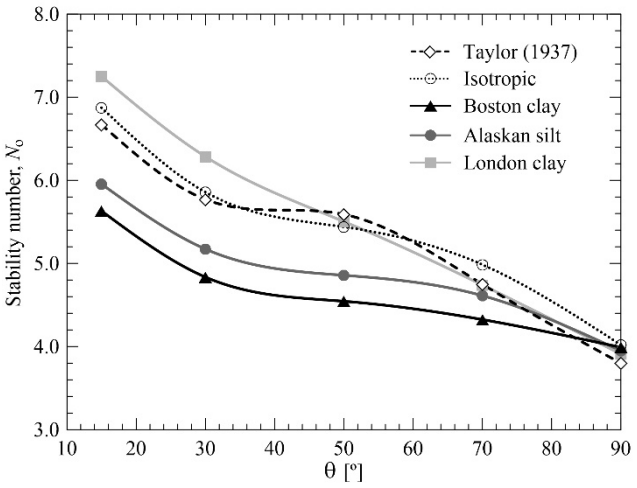

Figure 5. Variation of the stability number with slope inclination.

The failure mechanisms obtained are shown in Figure 6. As it is well known, the isotropic analysis transitions from a base mechanism, for low values of θ, to a toe mechanism, for high values of θ. A similar transition is observed in the anisotropic analyses although the toe mechanism is achieved for lower values of θ in the London clay compared to the isotropic analysis. The opposite occurs for the Boston clay, where larger values are required for the toe mechanism to develop. The failure mechanism for the Alaskan silt lies between the Boston clay and the isotropic analysis for a given value of θ.

By looking at the direction of σ_1 along the failure surface, the reason for the reduction of the effect of anisotropy with θ becomes evident. This is shown in Figure 7 for the isotropic analyses with θ = 15° and θ = 90°. In a base failure mechanism, the orientation σ_1 varies gradually along the failure surface from the sub-vertical to the sub-horizontal orientation. On the other hand, in the vertical cut the direction of σ_1 barely deviates from the sub-vertical orientation. This is the reason why the effects of anisotropy are negligible for a slope angle of 90º. Only one major principal stress direction is relevant.

The relative orientation between the major principal stress and the normal to the failure surface was found to be roughly equal to 45º throughout the surface and in all performed calculations. Therefore, it coincides with Roscoe's (1970) criterion.

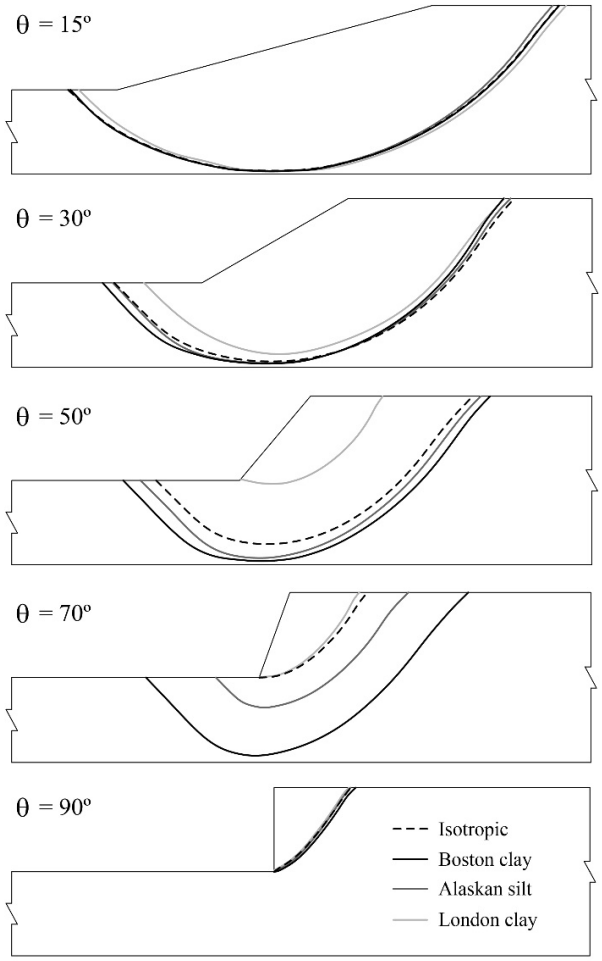

Figure 6. Failure surfaces obtained.

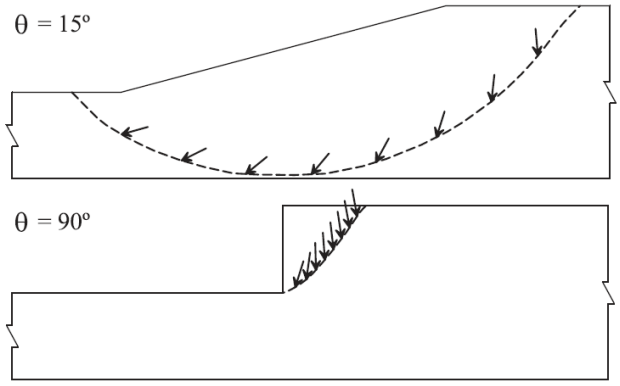

Figure 7. Direction of σ_1 along the failure surface for two isotropic analyses.

Analyses were also performed for the case with $\theta = 30°$, but with different bedding orientations α. Although less frequent, this condition may occur in nature due to cross-bedding or post-depositional deformations. The obtained stability numbers are shown in Figure 8. Values of $0 < \alpha < 90$ correspond to dip slopes while values of $90 < \alpha < 180$ correspond to anti-dip slopes. The failure mechanisms are not particularly dependent on the bedding orientation in this case and, therefore, they are not shown here. On the other hand, N_0 is significantly affected. Both the Boston clay and the Alaskan silt show N_0 values lower than the isotropic case for all bedding orientations. Nevertheless, dip slopes represent a more unfavourable situation. In contrast, the London clay shows N_0 values larger than the isotropic case for all bedding orientation except for a range in the anti-dip zone between 115° and 165°.

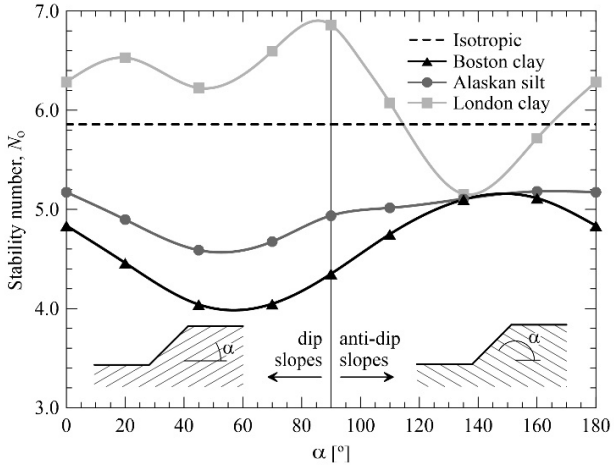

Figure 8. Variation of the stability number with bedding orientation.

5 FAILURE OF AN UNDERWATER SLOPE

In addition to the synthetic cases analysed in the previous section, a real case study was evaluated in order to stress the importance of including strength anisotropy in conventional stability calculations. It is the failure of a 30 m high underwater trench at the port of San Francisco (Duncan & Buchignani 1973). Figure 9 shows a cross-section of the slope before and after failure.

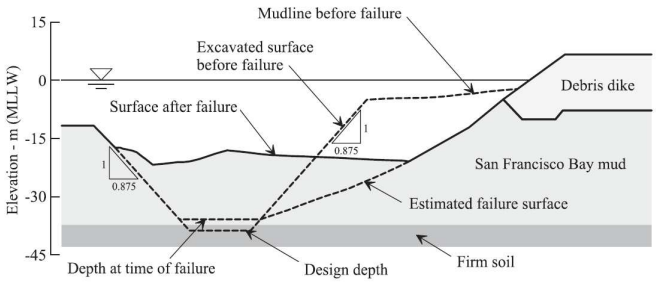

Figure 9. Cross-section of the failure (modified from Duncan 2000)

The original design calculations reported a FOS of 1.17 for the short-term condition, i.e. a stable slope (although with a rather low FOS). However, a few hours after excavation of a section about 150 long, a failure occurred, involving a 75 m long section of the trench. Later, a second failure took place involving an additional 60 m. Here, the possibility of explaining the observed failure by considering the undrained anisotropy of the San Francisco Bay mud was explored.

First, an analysis without anisotropy was performed to compare with the original stability calculations. The simplified geometry, mesh, and boundary conditions employed are depicted in Figure 10. The debris dike and the soil beneath it at the right of Figure 9 were not included in the analysis since preliminary calculation showed that the failure surface tended to pass beneath the dike. In the real slope failure, this did not occur most likely because the soil beneath the debris dike would have consolidated under the weight of the dike increasing its undrained strength.

The observed increase of undrained strength with depth was also included in the analysis; the profile reported by Duncan (2000) was employed.

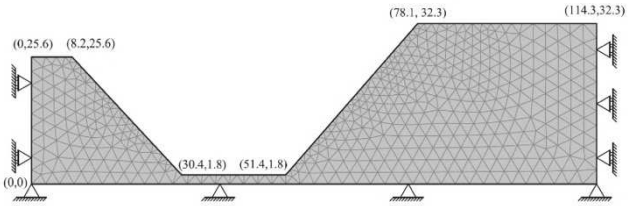

Figure 10. Geometry, mesh, and boundary conditions of the analysed case.

For the anisotropic analysis, data of the undrained strength variation with the loading direction of the San Francisco Bay mud from Lade & Kirkgard (2000) were employed. These results are depicted in Figure 11 (normalised with respect to the strength for $\delta = 0°$) together with the adjusted function and its parameters. The strength reduction method (Griffiths & Lane 1999) was again employed to derive the FOS.

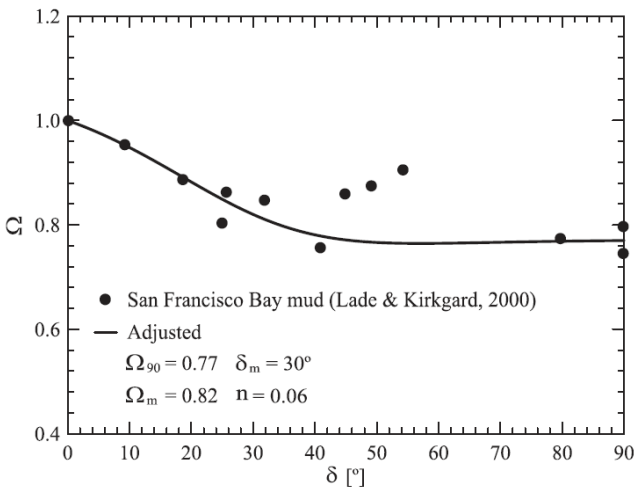

Figure 11. Observed (Lade & Kirkgard 2000) and computed normalised undrained strength distribution.

The obtained FOS and failure mechanisms (in terms of incremental displacements) are depicted in Figure12a and 12b for the isotropic and anisotropic cases respectively. For the isotropic case, a FOS of 1.18 was derived, confirming the original design value of 1.17. In addition, the failure mechanism is quite similar to the real surface, and it is practically identical to some revised calculations (Duncan et al. 2014). Therefore, it can be stated that this analysis is analogous to the original design computations.

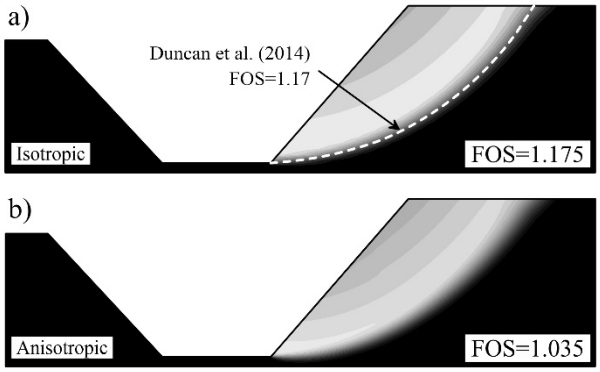

Figure 12. Failure mechanism and FOS for the (a) isotropic and (b) anisotropic analyses.

The anisotropic analysis is identical to the isotropic one, but it considers the strength distribution shown in Figure 11. In this case, the FOS is now very close to unity (1.035), i.e. very close to an incipient failure condition. Therefore, a more realistic FOS has been obtained just by including in the analysis the observed undrained strength anisotropy of the San Francisco Bay mud.

6 CONCLUSIONS

The FEM has been employed to study the effect of strength anisotropy on the undrained stability of cuts in clays. An anisotropic model has been described, able to account for the observed variation of the undrained strength observed in fine-grained soils. From the results, the following conclusions can be drawn:

- The effect of strength anisotropy decreases by increasing the inclination of the slope. This occurs because in the nearly planar toe mechanism, occurring in vertical or nearly vertical cuts, the orientation of σ_1 barely deviates from the sub-vertical direction and, therefore, the same strength operates than the isotropic case.
- For horizontal bedding, strength variations as those for the Boston clay and the Alaskan silt (Figure 3) always result in N_0 values lower than the isotropic case. For variations as the one shown by the London clay, anisotropy appears negligible for $\theta > 50°$and, for lower inclinations, N_0 values even higher than the isotropic case were obtained. Nevertheless, special care must be paid in the presence of pre-existing fissures, since the strength distribution obtained from non-fissured samples may not represent the strength of the soil mass and, therefore, the FOS may be lower than the isotropic case.
- Strength anisotropy has only a moderate effect on the obtained failure mechanism.

Finally, the introduction of strength anisotropy in the case study resulted in a more realistic FOS providing a satisfactory explanation to the observed failure.

7 REFERENCES

Arthur, J.R.F. Chua, K.S. & Dunstan, T. 1977. Induced anisotropy in a sand. *Géotechnique*, 27(1): 13-30.

Brinkgreve, R.B.J. Kumarswamy, S. & Swolfs, W.M. 2017. *PLAXIS 2D 2017*. Plaxis bv, Delft, Netherlands.

Chen, W.F. Snitbhan, N. & Fang, H.Y. 1975. Stability of slopes in anisotropic, nonhomogeneous soils. *Canadian Geotechnical Journal*, 12(1): 146-152.

Conesa, S. Mánica, M. Gens, A. & Huang, Y. 2018. Numerical simulation of the undrained stability of slopes in anisotropic fine-grained soils. *Geomechanics and Geoengineering*: 1-12.

Duncan, J.M. 2000. Factors of safety and reliability in geotechnical engineering. *Journal of Geotechnical and Geoenvironmental Engineering*, American Society of Civil Engineers, 126(4): 307-316.

Duncan, J.M. & Buchignani, A.L. 1973. Failure of underwater slope in San Francisco Bay. *Journal of the Soil Mechanics and Foundations Division*, 99(9): 687-703.

Duncan, J.M. Wright, S.G. & Brandon, T.L. 2014. *Soil strength and slope stability*. Wiley.

Fleming, L.N. & Duncan, J.M. 1990. Stress-deformation characteristics of Alaskan silt. *Journal of Geotechnical Engineering*, 116(3): 377-393.

Griffiths, D.V. & Lane, P.A. 1999. Slope stability analysis by finite elements. *Geotechnique*, 49(3): 387-403.

Lade, P.V. & Kirkgard, M.M. 2000. Effects of stress rotation and changes of b-values on cross-anisotropic behaviour of natural, K0-consolidated soft clay. *Soils and foundations*, 40(6): 93-105.

Nishimura, S. Minh, N.A. & Jardine, R.J. 2007. Shear strength anisotropy of natural London Clay. *Géotechnique*, 57(1): 49-62.

Roscoe, K.H. 1970. The influence of strains in soil mechanics. *Géotechnique*, 20(2): 129-170.

Seah, T.H. 1990. Anisotropy of resedimented Boston Blue Clay. Massachusetts Institute of Technology.

Skempton, A.W. & Hutchinson, J.N. 1969. Stability of natural slopes and embankment foundations. *Proceedings of the 7th international conference on soil mechanics and foundation engineering*, Mexico: 291-340.

Taylor, D.W. 1937. Stability of earth slopes. *Journal of the Boston Society of Civil Engineers*, 24: 197-246.

Zdravkovic, L. & Jardine, R.J. 2000. Undrained anisotropy of Ko-consolidated silt. *Canadian Geotechnical Journal*, 37(1): 178-200.